Article

Current Biology

Esco1 Acetylates Cohesin via a Mechanism Different from That of Esco2

Highlights

- Esco1 requires Pds5 to form sister chromatid cohesion
- Esco1 is recruited to cohesin complexes throughout interphase by Pds5
- Esco1 can acetylate SMC3 independently of DNA replication

Authors

Masashi Minamino, Mai Ishibashi, Ryuichiro Nakato, ..., Takashi Sutani, Masashige Bando, Katsuhiko Shirahige

Correspondence

mbando@iam.u-tokyo.ac.jp (M.B.), kshirahi@iam.u-tokyo.ac.jp (K.S.)

In Brief

Cohesion establishment at the DNA replication fork requires Esco1 and Esco2 acetyltransferases in humans. Minamino et al. show that Esco1, unlike Esco2, is recruited to chromatin-bound cohesin throughout interphase and acetylates cohesin independently of DNA replication.

Minamino et al., 2015, Current Biology *25*, 1694–1706
June 29, 2015
http://dx.doi.org/10.1016/j.cub.2015.05.017

CellPress

Current Biology
Article

Esco1 Acetylates Cohesin via a Mechanism Different from That of Esco2

Masashi Minamino,[1,2] Mai Ishibashi,[1,2] Ryuichiro Nakato,[1,2] Kazuhiro Akiyama,[1,2] Hiroshi Tanaka,[1] Yuki Kato,[1] Lumi Negishi,[3] Toru Hirota,[4] Takashi Sutani,[1,2] Masashige Bando,[1,2,*] and Katsuhiko Shirahige[1,2,5,*]

[1]Laboratory of Genome Structure and Function, Research Center for Epigenetic Disease, Institute of Molecular and Cellular Biosciences, University of Tokyo, 1-1-1 Yayoi Bunkyo-Ku, Tokyo 113-0032, Japan

[2]Graduate School of Agricultural and Life Sciences, University of Tokyo, 1-1-1 Yayoi Bunkyo-Ku, Tokyo 113-0032, Japan

[3]Laboratory of Cancer Stem Cell Biology, Research Center for Epigenetic Disease, Institute of Molecular and Cellular Biosciences, University of Tokyo, 1-1-1 Yayoi Bunkyo-Ku, Tokyo 113-0032, Japan

[4]Cancer Institute of the Japanese Foundation for Cancer Research (JFCR), 3-8-31 Ariake Koto-Ku, Tokyo 135-8550, Japan

[5]CREST, JST, K's Gobancho, 7, Gobancho, Chiyoda-ku, Tokyo 102-0076, Japan

*Correspondence: mbando@iam.u-tokyo.ac.jp (M.B.), kshirahi@iam.u-tokyo.ac.jp (K.S.)

http://dx.doi.org/10.1016/j.cub.2015.05.017

SUMMARY

Sister chromatid cohesion is mediated by cohesin and is essential for accurate chromosome segregation. The cohesin subunits SMC1, SMC3, and Rad21 form a tripartite ring within which sister chromatids are thought to be entrapped. This event requires the acetylation of SMC3 and the association of sororin with cohesin by the acetyltransferases Esco1 and Esco2 in humans, but the functional mechanisms of these acetyltransferases remain elusive. Here, we showed that Esco1 requires Pds5, a cohesin regulatory subunit bound to Rad21, to form cohesion via SMC3 acetylation and the stabilization of the chromatin association of sororin, whereas Esco2 function was not affected by Pds5 depletion. Consistent with the functional link between Esco1 and Pds5, Pds5 interacted exclusively with Esco1, and this interaction was dependent on a unique and conserved Esco1 domain. Crucially, this interaction was essential for SMC3 acetylation and sister chromatid cohesion. Esco1 localized to cohesin localization sites on chromosomes throughout interphase in a manner that required the Esco1-Pds5 interaction, and it could acetylate SMC3 before and after DNA replication. These results indicate that Esco1 acetylates SMC3 via a mechanism different from that of Esco2. We propose that, by interacting with a unique domain of Esco1, Pds5 recruits Esco1 to chromatin-bound cohesin complexes to form cohesion. Furthermore, Esco1 acetylates SMC3 independently of DNA replication.

INTRODUCTION

Sister chromatid cohesion conferred by the cohesin complex is essential for accurate chromosome segregation [1, 2]. Cohesin complex, which consists of structural maintenance of chromosomes 1 (SMC1), SMC3, and Rad21, is proposed to topologically embrace both sister chromatids [3]. Rad21 binds to the fourth cohesin core subunit, stromal antigen (SA), which contains two paralogs (SA1 and SA2). Rad21 and SA proteins are further associated with several other factors, including Pds5, Wapl, and sororin, which enable cohesin rings to build, maintain, and dissolve cohesion during cell-cycle progression [4, 5].

Cohesin is loaded onto chromosomes prior to DNA replication, but recent reports suggest that cohesin loading alone is not sufficient for cohesin-dependent tethering of replicated chromosomes. The loaded cohesin requires an additional "establishment" step that involves the acetylation of a pair of lysine residues within SMC3 by the evolutionarily conserved cohesin acetyltransferases (CoATs) (Eco1 in budding yeast and Esco1 and Esco2 in human) [6–15]. In metazoans, cohesion establishment also requires association with sororin during DNA replication to antagonize cohesin-release factor Wapl, and SMC3 acetylation facilitates, but is not sufficient for, the association [16, 17].

The regulation of CoAT function has been explored in budding yeast. Cohesion establishment occurs in S phase, when SMC3 is acetylated [12, 13, 18, 19]. Eco1 transiently binds to chromosomes during S phase in a manner that depends on a physical interaction between Eco1 and PCNA [20], which is believed to enable Eco1 to establish cohesion specifically between identical sister chromatids at the DNA replication fork, although Eco1 movement along chromosomes has not been directly observed [19].

Unlike yeast, human SMC3 is acetylated before the recruitment of PCNA [21], and there are two Eco1 orthologs, Esco1 and Esco2, which contain a vertebrate-specific divergent N terminus followed by an evolutionarily conserved acetyltransferase domain [14, 15]. Whereas both Esco1 and Esco2 are able to acetylate SMC3 at K105 and K106 [7, 17], these Esco proteins are differently regulated in humans. Esco2, like budding yeast Eco1, binds to chromosomes only during S phase [15]. In contrast, Esco1 is expressed throughout the cell cycle [15]. Importantly, neither Esco protein is able to fully compensate for loss of the other, suggesting that the functions of these two proteins are not completely redundant [15]. However, little is known about the specificity of the functional mechanisms of the two Esco proteins.

Here, we used genetic, biochemical, and genomic studies to demonstrate that Pds5 depletion specifically abolishes the

Esco1-dependent cohesion pathway, that Pds5 interacts exclusively with Esco1, and that Esco1 localizes to cohesin localization sites throughout interphase by interacting with Pds5. Intriguingly, Esco1 was able to acetylate SMC3 independently of DNA replication. These findings led us to propose that Esco1 acetylates SMC3 via a mechanism different from that of Esco2 and that, by interacting with Esco1, Pds5 recruits Esco1 to chromatin-bound cohesin complexes to form cohesion.

RESULTS

Esco1 Requires Pds5 to Acetylate SMC3

To examine the relative contributions of the two Esco proteins to SMC3 acetylation during cell-cycle progression, we depleted these proteins from HeLa cells using small interfering RNA (siRNA) (Figure S1A). The cells were synchronized in S phase or G1 phase using double-thymidine block and release (Figure S1B). We then analyzed the SMC3 acetylation with an antibody that specifically recognizes SMC3 when K106 or both K105 and K106 are acetylated (Figures 1A and 1B) [17]. Depletion of either Esco1 or Esco2 reduced SMC3 acetylation by ~14% and ~31%, respectively, and depletion of both of these enzymes resulted in an ~86% reduction in acetylation in S phase (Figure 1A) [17]. In contrast, SMC3 acetylation was only slightly reduced by Esco2 depletion (by ~4%) but substantially reduced by Esco1 depletion (by ~84%) in G1 phase (Figure 1B). Crucially, the magnitude of this reduction is similar to that observed after simultaneous depletion of Esco1 and Esco2 (~90% reduction). These results indicated that SMC3 acetylation depends almost entirely on Esco1 in G1 but requires both Esco1 and Esco2 in S phase.

Budding yeast Eco1 is known to physically interact with Pds5 [22]. Recent studies have reported that SMC3 acetylation requires Pds5 in budding and fission yeast, and it requires Pds5A and Pds5B in mouse embryonic fibroblasts [23–25], although the molecular mechanisms underlying this requirement are not clear. To test whether this aspect of Pds5 is conserved in humans, we depleted the two Pds5 paralogs and analyzed SMC3 acetylation (Figures 1A, 1B, S1A, and S1B). Simultaneous depletion of the two Pds5 proteins reduced SMC3 acetylation in S phase by ~32%, and we observed a more substantial (~71%) reduction when these cells were synchronized in G1 phase. In G1 phase, individual depletion of Pds5A and Pds5B reduced the levels by ~43% and ~49%, respectively. These results indicated that human Pds5A and Pds5B regulate this modification, at least partially, in a non-redundant manner. To examine the functional overlap of Pds5 with the Esco proteins, we simultaneously depleted Pds5 and either Esco1 or Esco2 and analyzed SMC3 acetylation (Figure 1A). Depletion of Pds5A and Pds5B only slightly reduced SMC3 acetylation upon Esco1 depletion, but co-depletion of Esco2, Pds5A, and Pds5B resulted in a synergetic reduction. Crucially, the SMC3 acetylation level in cells depleted of Pds5A, Pds5B, and Esco2 was similar to that observed in Esco1 and Esco2 co-depleted cells. These results indicated that Pds5A and Pds5B are essential for Esco1-dependent SMC3 acetylation.

To address whether the lack of Esco1-dependent SMC3 acetylation in Pds5-depleted human cells is caused by defective de novo acetylation or by a failure to block deacetylation by the SMC3 deacetylase HDAC8, we depleted Esco1 or both Pds5A and Pds5B in asynchronous cells and measured SMC3 acetylation in the presence of the HDAC8 inhibitor PCI-34051 (hereafter PCI). SMC3 acetylation increased rapidly in the presence of PCI (Figure 1C), as reported [26], but was blocked upon individual depletion of Esco1 and Pds5, suggesting that Pds5 promotes de novo SMC3 acetylation.

Esco1 Can Acetylate SMC3 after DNA Replication

To test whether Esco1 acetylates SMC3 after DNA replication, cells depleted of Esco1, Esco2, or Pds5 were arrested in G2/M phase by the Cdk1 inhibitor RO3306 (Figures 1D and 1E). We further treated these cells with PCI for 2 hr and found that PCI increased SMC3 acetylation levels in G2/M-arrested cells, suggesting de novo SMC3 acetylation after DNA replication. This increase was unaffected by Esco2 depletion, but it was prevented in cells depleted of Esco1 or Pds5. Postreplicative de novo SMC3 acetylation therefore requires Esco1 and Pds5.

Esco1 Requires Pds5 to Stabilize the Chromatin Association of Sororin

We tested whether sororin is involved in regulation of SMC3 acetylation (Figure S2A). Individual depletion of Esco1, Esco2, and sororin only slightly affected SMC3 acetylation in G2 (<8% reduction) [17]. Interestingly, co-depletion of sororin and Esco1, unlike co-depletion of sororin and Esco2, produced a synergetic reduction (~48%), indicating that sororin depletion reduces Esco2 mediated-SMC3 acetylation in G2. We further found that SMC3 acetylation levels in cells depleted of Esco1 and sororin were substantially increased by PCI (Figures S2B and S2C). We concluded that Esco2, at least in part, retains its acetyltransferase activity in sororin-depleted cells, but sororin is essential for Esco2-mediated SMC3 acetylation in G2.

We then analyzed the contribution of Esco1, Esco2, and Pds5 to the recruitment of Wapl and sororin. We performed biochemical fractionation experiments with extraction buffer containing 100 mM NaCl and observed little effect of depletion of Esco proteins on the amount of Wapl on chromatin, whereas Pds5 depletion reduced Wapl on chromatin (Figure S2D). The simultaneous depletion of both Esco proteins had no major effect on the amount of sororin on chromatin with the extraction buffer containing 100 mM NaCl (Figure S2D), but it resulted in a reduction of sororin on chromatin with 250 mM NaCl (Figures 2A and S2E), indicating the promotion of chromatin association of sororin by Esco1 and Esco2 [17]. Interestingly, the individual depletion of Esco2, unlike that of Esco1, reduced sororin on chromatin (Figures 2A and S2F), indicating that Esco2 has a non-redundant role in stabilizing the chromatin association of sororin, although both Esco proteins contribute to the process. Pds5 depletion had little effect on the chromatin association of sororin. Interestingly, depletion of both Esco2 and Pds5 reduced sororin on chromatin to a similar extent as the depletion of the two Esco proteins, whereas the simultaneous depletion of Esco1 and Pds5 had little effect (Figure 2A). These results indicated that Esco1 and Pds5 stabilize the chromatin association of sororin in the same pathway.

To validate the functional overlap of Esco1 with Pds5, we prepared mitotic chromosome spreads from cells that had been depleted of these proteins and analyzed the resulting chromosome morphology. Depletion of either Esco1 or Esco2 slightly

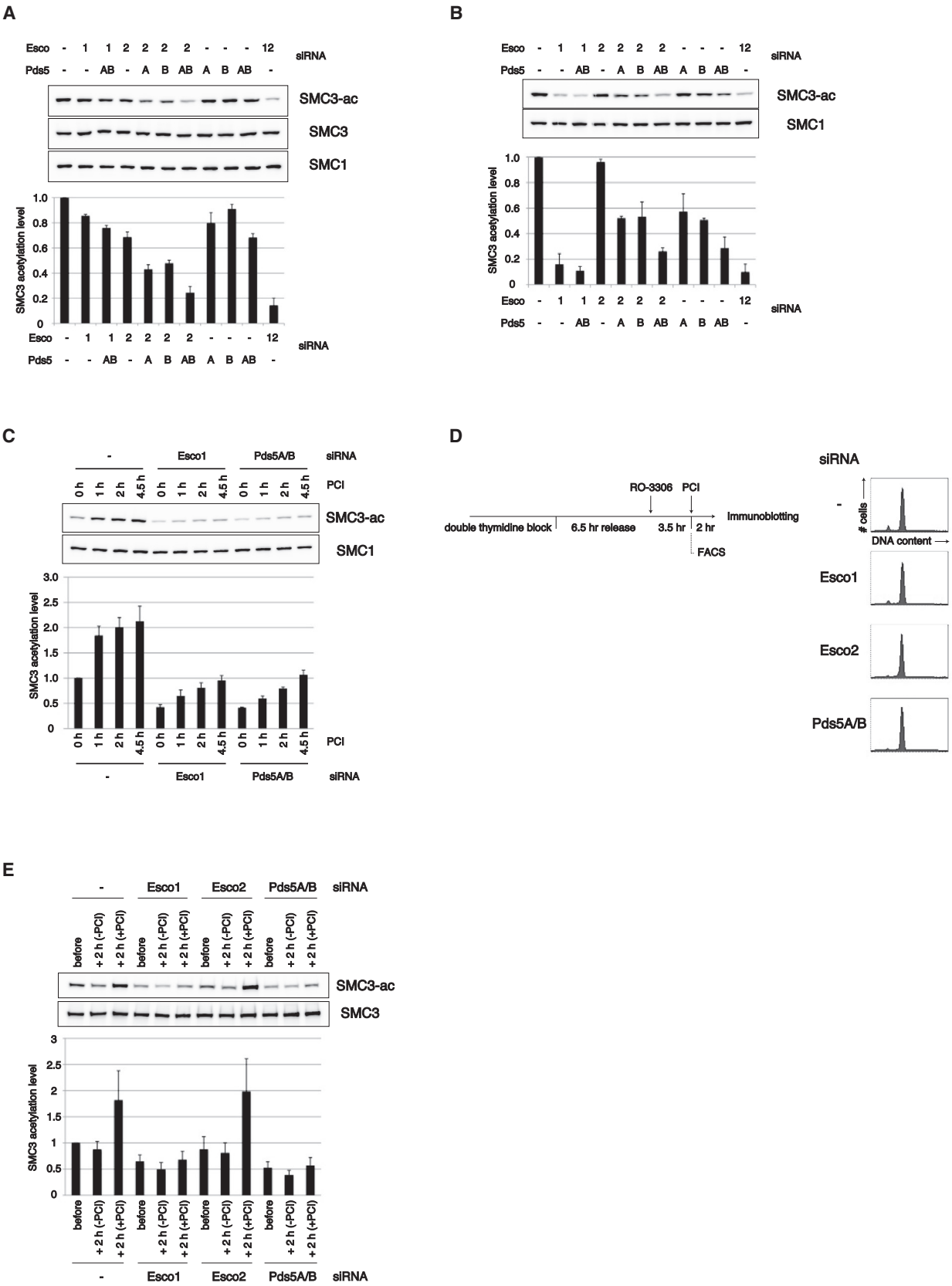

(legend on next page)

increased the frequency of cells exhibiting precocious separation of sister chromatid, and we observed a further increase when both Esco proteins were depleted (Figure 2B), confirming a previous report [15]. The simultaneous depletion of Esco1, Pds5A, and Pds5B produced no additive defects in the cohesion pathway. Interestingly, however, Esco2 depletion resulted in an enhanced synergetic defect upon depletion of Pds5A and Pds5B. Moreover, the triple depletion of Esco2, Pds5A, and Pds5B caused a massive precocious separation of sister chromatids. This defect was similar in magnitude to that observed after simultaneous depletion of Esco1 and Esco2. These results, along with our SMC3 acetylation data, indicated that Pds5A and Pds5B are both required for Esco1 to establish cohesion. Whereas Pds5 depletion efficiently prevented Esco1 function, it is possible that the amount of Pds5 left after depletion is sufficient to sustain chromatin association of sororin and/or to mediate Esco2 function (Figure S1A).

Esco1 Physically Interacts with Pds5 via a Highly Conserved Region

We tested whether Esco proteins physically interact with the cohesin components. Virtually no interaction was detectable between Esco proteins and SMC3, SA1, or SA2, whereas both Esco1 and Esco2 weakly interacted with Rad21 (Figures S3A–S3C; data not shown). Interestingly, FLAG-tagged Esco1 (FLAG-Esco1) coimmunoprecipitated with considerable amounts of Pds5A, whereas Pds5A was hardly detectable upon coimmunoprecipitation with FLAG-tagged Esco2 (FLAG-Esco2; Figure 3A), which is consistent with the observed functional overlap between Esco1 and Pds5 (Figure 1). To locate the Pds5-binding region in Esco1, we generated partial fragments of Esco1 and measured the ability of each fragment to interact with Pds5A (Figures S3D and S3E). This mapping experiment indicated that the region containing residues 263–344 is essential for the interaction of Esco1 with Pds5A. Interestingly, amino acid sequence comparison showed that this region contains highly conserved sequences among Esco1 orthologs (Figure 3B). To test whether this domain plays a direct role in interacting with Pds5, we took a site-directed mutagenesis approach to generate several mutants of full-length Esco1 in which triplet sequences within the Pds5-binding domain were replaced with three alanine residues (termed 3A; Figure 3C). We then analyzed the ability of each mutant to interact with Pds5A and found that 3A mutation of two regions, namely residues 302–304 and 315–317, attenuated the interaction, whereas 3A mutation at other sites had no effect. Esco1 also interacts with Pds5B, and this interaction was also prevented by the 302–304 3A mutation (Figure 3D), whereas this mutation hardly affected the Esco1-Rad21 interaction (Figure S3C). These results indicated that Esco1 presumably interacts with Rad21 and Pds5 through different Esco1 regions and that a domain evolutionarily conserved among vertebrates is responsible for the interaction between Esco1 and Pds5. Based on these experiments, we hereafter refer to residues 263–344 of Esco1 as the Pds5-binding (PDB) domain. We also generated partial fragments of Pds5A and tested whether these fragments interact with Esco1. We found that neither the N-terminal (residues 1–200) nor C-terminal (residues 1,191–1,337) regions of Pds5A are essential for interaction with Esco1 (data not shown).

The PDB Domain of Esco1 Is Indispensable for Cohesion

To address whether the PDB domain of Esco1 is required for its function, we constructed HeLa cell lines stably expressing siRNA-resistant versions of wild-type or 302–304 3A mutant (hereafter 3A mutant) GFP-tagged Esco1 (GFP-Esco1) (Figure 4A). We depleted either only endogenous Esco1 or both endogenous Esco1 and Esco2 from these cells (Figures 4A, 4B, and S4A). As expected, depletion of Esco1 and simultaneous depletion of Esco1 and Esco2 reduced SMC3 acetylation and ectopic expression of wild-type Esco1 largely rescued the reduction. However, the Esco1 3A mutant failed to rescue this loss of SMC3 acetylation. Therefore, the PDB domain is essential for Esco1 to acetylate SMC3.

To test whether the Esco1 3A mutant retains acetyltransferase activity, we prepared Sf9 insect cells in which SMC3 was coexpressed with wild-type or 3A mutant Esco1 (Figure 4C). SMC3 was acetylated by wild-type Esco1, and this reaction is abolished by a G768D mutation in the conserved acetyltransferase domain of Esco1, indicating that our measurements of SMC3 acetylation were sensitive enough to detect changes in the acetyltransferase activity of Esco1. The Esco1 3A mutant acetylated SMC3 as efficiently as wild-type Esco1 (Figure 4C). Moreover, SMC3 acetylation by Esco1 is not increased by Pds5A expression (Figure S4B). We conclude that Pds5 is not essential

Figure 1. Pds5 Depletion Specifically Abolishes Esco1-Dependent SMC3 Acetylation

(A and B) Immunoblotting of lysates from untransfected (−) cells and cells transfected with the indicated siRNAs. HeLa cells were transfected with the siRNAs for 2 days and were then synchronized in S phase (A) and G1 phase (B) by double-thymidine block and release. Total levels of SMC1 and SMC3 served as a loading control. SMC3-ac levels in cells transfected with siRNAs were normalized to SMC1 and untransfected cells. The experiments were performed three times independently. The representative immunoblotting results (upper) along with the mean and SD of three experiments (lower) are shown. SMC3-ac, acetylated SMC3.

(C) Immunoblotting of lysates from untransfected (−) cells and cells transfected with Esco1 siRNA or with both Pds5A and Pds5B siRNAs for 2 days in the presence or absence of the HDAC8 inhibitor PCI. Total levels of SMC1 served as a loading control, and SMC3-ac levels were normalized to SMC1 and the 0 hr time point of untransfected cells. The experiment was performed three times independently, and the representative immunoblotting results (upper) along with the mean and SD of three experiments (lower) are shown.

(D) Schematic representation of the experimental protocol (left). Untransfected HeLa cells (−) or HeLa cells transfected for 2 days with siRNAs specific for Esco1, Esco2, or both Pds5A and Pds5B were arrested in G2/M phase by the Cdk1 inhibitor RO3306 after synchronization via double-thymidine block and release. PCI was then added, and these cells were further incubated for 2 hr in the presence of RO3306. Cells were collected at the time of PCI addition to obtain cell-cycle profiles by fluorescence-activated cell sorting (FACS) (right).

(E) Immunoblotting of lysates from cells in (D). G2/M-arrested cells were collected before (before) or after incubation for 2 hr in the presence (+2h [+PCI]) or absence of PCI (+2h [−PCI]). The experiments were performed three times independently. The representative immunoblotting results (upper) along with the mean and SD of three experiments (lower) are shown. See also Figure S1.

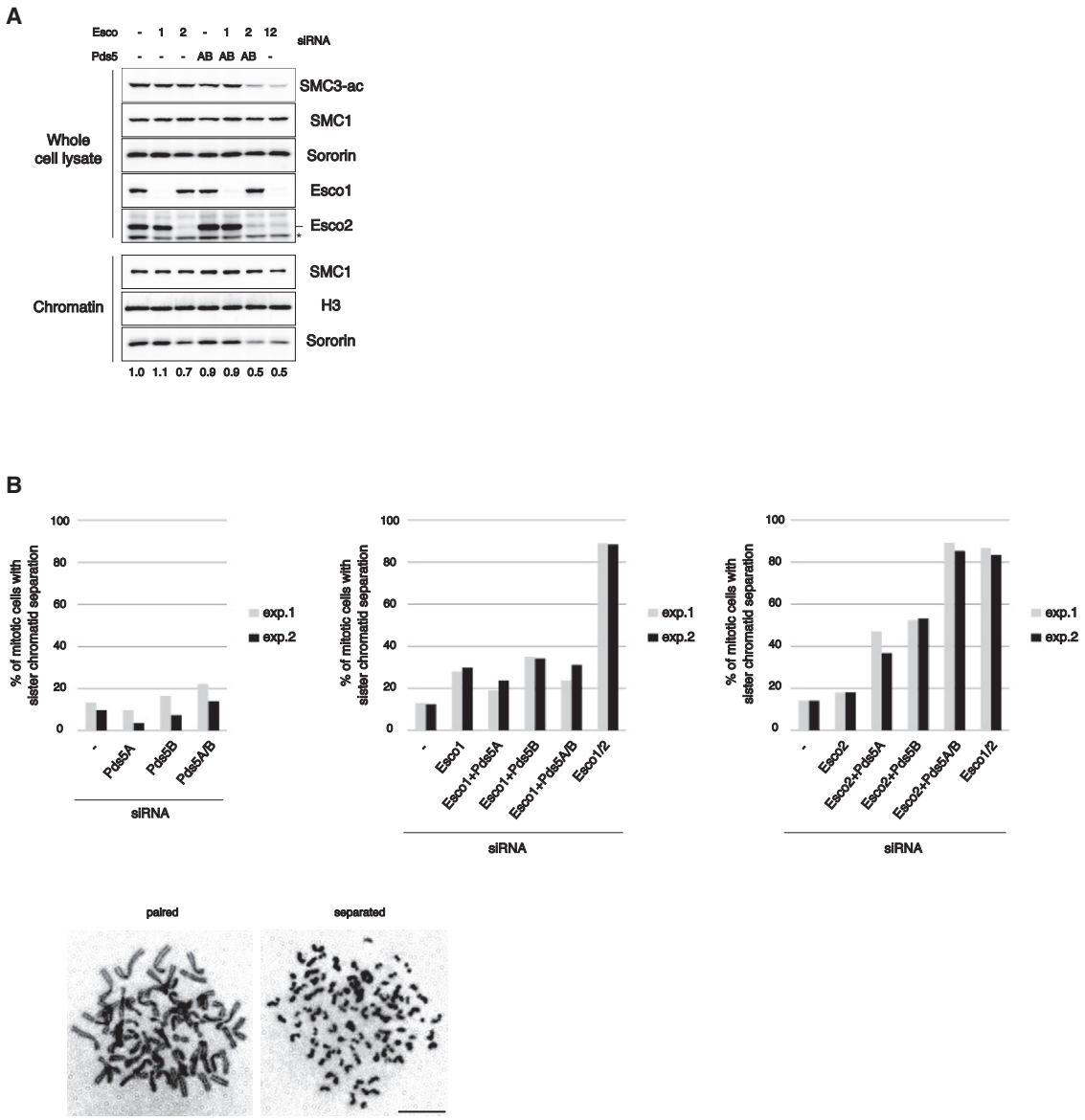

Figure 2. Esco1 and Pds5 Promote the Chromatin Association of Sororin in the Same Pathway

(A) Chromatin fractionation of untransfected (−) cells and cells transfected with the indicated siRNAs. Cells that had been depleted of Esco and Pds5 were synchronized in S phase by double-thymidine block and release. Cells were transfected with the Esco1 and Pds5 siRNAs before the first thymidine arrest and Esco2 siRNA after the release from the first thymidine arrest. Histone H3 served as a loading control of the chromatin-enriched fraction (chromatin). Numbers beneath sororin bands indicate quantification of sororin levels on chromatin normalized to histone H3 (H3) levels and untransfected cells. The asterisk indicates nonspecific signals.

(B) Quantification of the percentage of mitotic HeLa cells exhibiting separated sister chromatids after combinational depletion of Pds5A and Pds5B (left), Esco1 and Pds5 (middle), and Esco2 and Pds5 (right). The experiments were performed twice independently, and representative Giemsa-stained mitotic chromosome spreads of paired and separated sister chromatids after siRNA transfection (lower) are shown. One hundred cells per RNAi experiments were classified into two groups in each experiment. Paired and separated chromatids were obtained from untransfected cells and cells transfected with both Esco1 and Esco2 siRNAs, respectively. Hypercondensation phenotype, which is observed in mitotic chromosomes obtained from cells depleted of Esco1 and Esco2, may not be due to depletion of Esco1 and Esco2, because this phenotype was observed in separated chromosomes obtained from untransfected cells (data not shown). Bar, 10 μm (see also Figure S2).

for acetyltransferase activity of Esco1 and defective SMC3 acetylation in the Esco1 302–304 3A mutant cells may not be due to the loss of acetyltransferase activity of this mutant.

To further address whether the PDB domain of Esco1 contributes to cohesion, we prepared mitotic chromosome spreads from cells carrying the Esco1 3A mutant in place of endogenous Esco1 (Figure 4D). Depletion of both Esco proteins caused a pervasive precocious separation of sister chromatid, which was largely rescued by ectopic wild-type Esco1, as expected. However, the Esco1 3A mutant was less effective in this rescue.

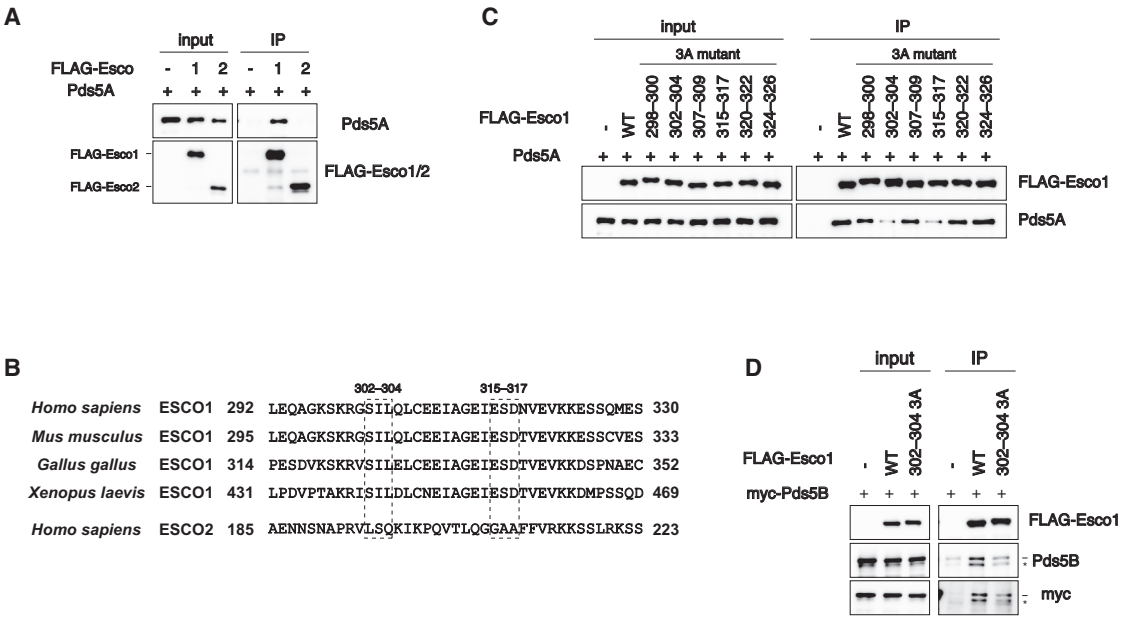

Figure 3. Pds5 Preferentially Interacts with Esco1

(A) Interaction of Pds5A with Esco proteins. FLAG-Esco1 or FLAG-Esco2 was coexpressed with Pds5A in Sf9 insect cells using baculoviruses. Immunoprecipitates (IPs) obtained from cell lysates using anti-FLAG beads and input fractions were analyzed by immunoblotting.

(B) Conserved sequences within the Pds5-binding domain of orthologous Esco1 proteins from different species and Esco2 of humans. The two triplet-residue sequences essential for Pds5 interaction are indicated by dashed rectangles.

(C) Interaction of Pds5A with a series of Esco1 mutants. FLAG-Esco1 wild-type (WT) or mutants were coexpressed with Pds5A in Sf9 insect cells and then precipitated with anti-FLAG beads. The precipitates along with input fractions were analyzed by immunoblotting.

(D) Interaction of Pds5B with Esco1. Myc-tagged Pds5B (myc-Pds5B) was coexpressed with FLAG-Esco1 WT or the Esco1 302–304 3A mutant in Sf9 insect cells with baculovirus. Immunoprecipitates obtained from cell lysates using anti-FLAG beads were analyzed by immunoblotting. The asterisks indicate possible degradation products of myc-Pds5B (see also Figure S3).

Taken together, we concluded that the PDB domain of Esco1 is indispensable for cohesion.

Esco1 Colocalizes with Cohesin throughout Interphase

We next analyzed the distribution of Esco1 on chromosomes. Because our Esco1 antibody was not effective for chromatin immunoprecipitation (ChIP) (data not shown), we prepared HeLa cells expressing siRNA-resistant versions of GFP-Esco1 at levels comparable to that of endogenous Esco1, and we depleted only the endogenous Esco1. Immunoblotting revealed that endogenous Esco1 was largely replaced by the GFP-Esco1 (Figure 5A). We then carried out a ChIP-sequencing (ChIP-seq) assay with anti-GFP (Figures 5B and S5A) and identified 12,386 and 11,797 GFP-Esco1 sites in G1 and G2, respectively (Table S1). Depletion of GFP-Esco1 eliminated the GFP-Esco1 ChIP-qPCR signals (Figure 6B), suggesting that most, if not all, of the sites identified in the ChIP-seq were specific for Esco1. The localization of endogenous Rad21 and Pds5A were also assessed to map the cohesin localization sites (Figure 5B); 27,333 and 24,592 localization sites for Rad21 and Pds5A, respectively, were identified in G1; and 29,958 and 24,127 Rad21 and Pds5A localization sites, respectively, were identified in G2 (Table S1). We classified the localization sites of GFP-Esco1, Rad21, and Pds5A relative to genes (Figure S5B) and observed no major enrichment of GFP-Esco1 localization sites in specific regions, although GFP-Esco1 localization sites were slightly over-represented in upstream and downstream region of genes (14% and 12% of GFP-Esco1 localization sites in G1 and G2, respectively) compared to their frequency in the genome (8%). Similarly, Rad21 and Pds5A did not preferentially localize to specific regions, whereas most of yeast cohesin localization sites on chromosome arms are regions of convergent transcription [27, 28]. Notably, we observed a high degree of overlap among GFP-Esco1, Rad21, and Pds5A in both G1 and G2 (Figures 5B, 5C, S5C, and S5D), with most of the GFP-Esco1, Rad21 [29], and Pds5A sites being identical between these two phases (Figures 5B, 5D, and S5E). Moreover, GFP-Esco1, like cohesin, dissociated from these sites in prometaphase cells (Figures 5B, 5D, and S5E) [29–31]. Consistently, time course analysis of GFP-Esco1 localization indicated that a considerable amount of GFP-Esco1 localized to cohesin sites throughout DNA replication and dissociated from these sites in prometaphase (Figures 5E and S5F). We concluded that Esco1 colocalizes with cohesin throughout interphase.

Pds5 Recruits Esco1 to Cohesin Localization Sites

We then tested whether chromatin loading of Esco1 depends on cohesin. The amount of Esco1 on chromatin was not affected by depletion of Pds5 or Rad21 (Figure S6A), and 302–304 3A mutant Esco1 bound to chromatin as efficiently as wild-type (Figure S6B), indicating that cohesin had no major effect on the association of Esco1 with chromatin, at least under these

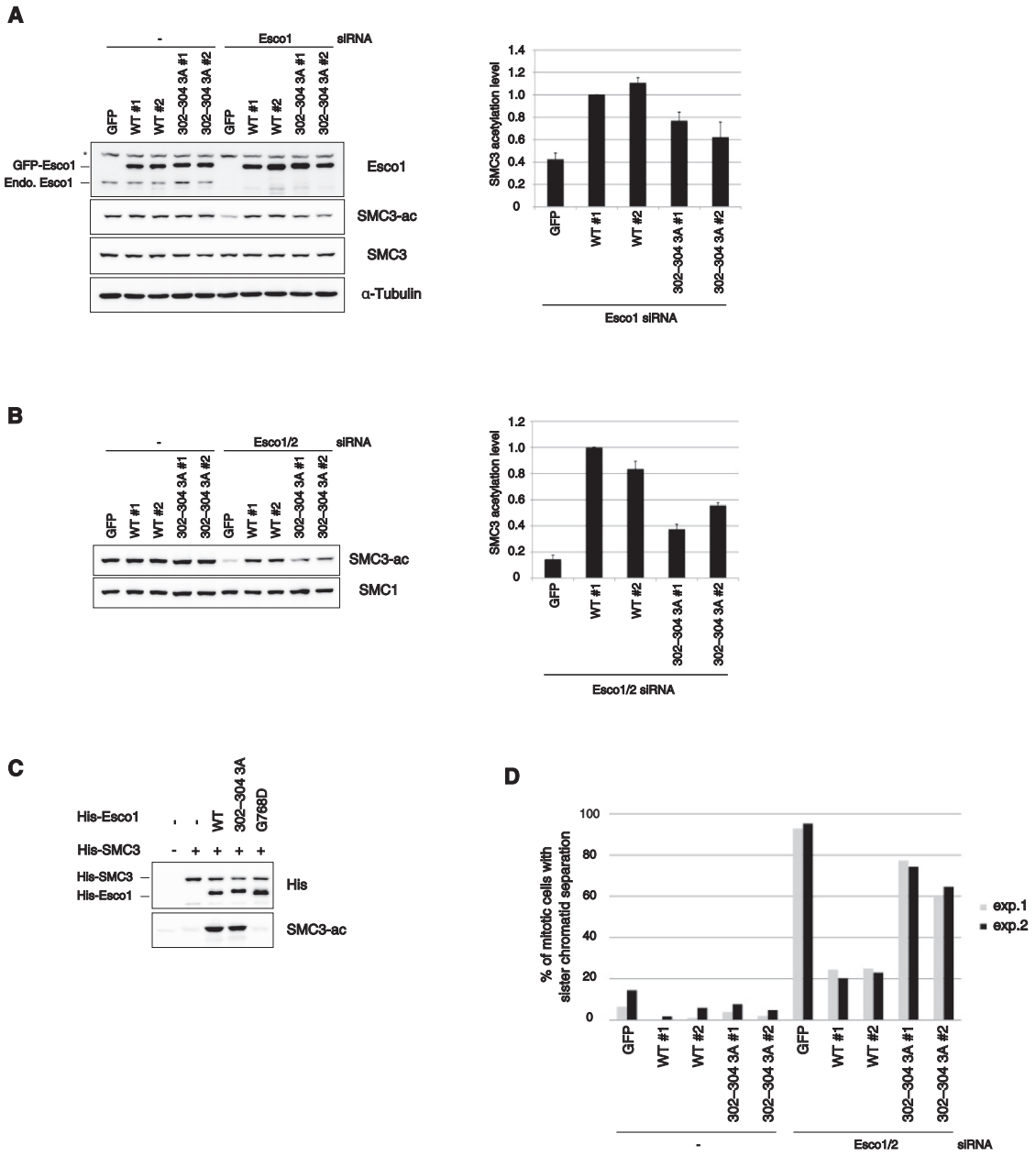

Figure 4. The Pds5-Binding Domain of Esco1 Is Essential for Sister Chromatid Cohesion

(A and B) (Left) Immunoblotting analysis of lysates from cells carrying the Esco1 302–304 3A mutant in the place of endogenous (Endo.) Esco1. HeLa cells were generated that stably expressed siRNA-resistant versions of wild-type GFP-Esco1 (WT) or GFP-Esco1 302–304 3A mutant. Two clones for each line were not transfected (–) or transfected with Esco1 siRNA (A) or with both Esco1 and Esco2 siRNAs (B) for 2 days. The cells were grown asynchronously (A) or synchronized in S phase by double-thymidine block and release (B). Lysates from these cells were then analyzed by immunoblotting. Tubulin is shown as a loading control (A). The asterisk indicates nonspecific signals. (Right) Quantification of SMC3-ac levels in cells carrying the Esco1 302–304 3A mutant in the place of Endo. Esco1. The experiments on the left were repeated twice, and SMC3-levels were normalized to cells expressing wild-type GFP-Esco1 (WT #1). The mean and SD of three independent experiments are shown.

(C) Measurement of acetyltransferase activity of 302–304 3A mutant Esco1. His-tagged SMC3 (His-SMC3) was coexpressed with WT, 302–304 3A, or G768D mutant His-tagged Esco1 (His-Esco1) in insect cells using the baculovirus expression system. Lysates from these cells were then analyzed by immunoblotting.

(D) Quantification of the percentage of mitotic HeLa cells exhibiting separated sister chromatids after the replacement of endogenous Esco1 with GFP-Esco1 WT or the GFP-Esco1 302–304 3A mutant. Cells were not transfected or transfected with both Esco1 and Esco2 siRNAs for 2 days and were examined by chromosome spreads and Giemsa staining. The experiments were performed twice independently, and 100 cells per RNAi experiments were classified into two groups in each experiment (see also Figure S4).

assay conditions. This is consistent with a previous report that an N-terminal fragment of Esco1, which was shown previously to efficiently bind to chromatin, does not contain the PDB domain [15].

We then utilized cells overexpressing GFP-Esco1 to address whether Esco1 localization is regulated by cohesin (Figure S6C). Our ChIP-seq analysis clearly showed that Pds5 depletion substantially disrupted the localization of GFP-Esco1 (Figure 6A). We further measured the amount of GFP-Esco1 by ChIP-qPCR at cohesin localization sites in cells depleted of Pds5 or Rad21. Depletion of Pds5 or Rad21 reduced the amount of GFP-Esco1 at cohesin localization sites (Figures 6B and S6D). It is possible that the residual amount of Esco1 at cohesin localization sites seen in our assay was due to incomplete depletion of Pds5 or Rad21 (Figures 1A and S6A).

We also observed that Rad21 depletion reduced Pds5 on chromatin (Figure S6A), as reported [32]. In contrast, Rad21 localization was only slightly affected by Pds5 depletion (Figure 6B), which prompted us to test whether Esco1 localization depends on the interaction with Pds5. We then assessed the localization of wild-type GFP-Esco1 and the GFP-Esco1 3A mutant (Figures 6C and 6D). The enrichment of Esco1 at cohesin localization sites was substantially reduced with the 3A mutant, indicating that Esco1 is recruited to cohesin localization sites via its PDB domain.

DISCUSSION

In the current model, cohesion establishment by Esco1 and Esco2 depends on SMC3 acetylation, which facilitates the chromatin association of sororin [17]. Here, we showed that depletion of the two Pds5 paralogs, Pds5A and Pds5B, prevented Esco1 from promoting the two events, whereas it did not affect Esco2 function. We propose that Esco1 and Esco2 acetylate SMC3 via different mechanisms and that Esco1 requires Pds5 to establish cohesion. Our biochemical analyses further showed that Pds5 preferentially interacts with Esco1 and that this interaction depends on an Esco1-specific domain, thus explaining how Pds5 discriminates Esco1 from Esco2 to regulate SMC3 acetylation. The interaction of Esco1 with Pds5 was found to be essential for Esco1 to localize to cohesin localization sites and for cohesion, suggesting that Pds5 recruits Esco1 to cohesin to establish cohesion.

Unexpectedly, Esco1 localization sites, which overlap with cohesin localization sites, are identical between G1 and G2. Whereas budding yeast Eco1 localizes to the DNA replication fork in early S phase cells arrested by replication inhibitor hydroxyurea [33], our results suggest that human Esco1 is recruited to cohesin localization sites independently of DNA replication, which is consistent with our finding of DNA replication-independent SMC3 acetylation by Esco1. Although Esco1 acetylates SMC3 independently of DNA replication, cohesion establishment should occur specifically at DNA replication fork in humans, because sororin loading, an additional requirement for cohesion establishment, is coupled to DNA replication [17]. However, it is possible that postreplicative SMC3 acetylation by Esco1 contributes to the reinforcement of cohesion after cohesion establishment [33–36], although this hypothesis will need to be verified in the future. It also will be interesting to test whether replication-independent SMC3 acetylation is involved in transcriptional regulation [37].

Esco2 has a larger role than Esco1 in stabilizing chromatin association of sororin, whereas the SMC3 acetylation level in cells depleted of Esco2 was similar to that observed in Esco1-depleted cells, suggesting that Esco2 stabilizes chromatin association of sororin through an unidentified event(s) in addition to SMC3 acetylation. We also found that sororin is essential for Esco2-mediated SMC3 acetylation in G2. Because Esco2 appears to largely retain its acetyltransferase activity in sororin-depleted cells, we suppose that Esco2 acetylates SMC3 independently of sororin but the acetylated cohesin is quickly reversed by HDAC8 in sororin-depleted cells, where cohesin is dynamically bound to chromatin [38]. These findings further suggest that SMC3 acetylation and chromatin association of sororin should be coupled at the DNA replication fork in the Esco2-dependent cohesion establishment pathway.

Specific loss of cohesion at pericentric heterochromatin is observed in Esco2-deficient mouse embryonic fibroblasts and in cells isolated from patients of Roberts syndrome with mutations in Esco2 [16, 39]; however, we have not observed such defect in Esco2-depleted HeLa cells so far. This may be explained by a difference in chromosome architecture between these cell types. A recent study also reported that the amount of chromatin-bound Esco2 is not altered but its specific localization pattern is partially lost in Pds5-deficient mouse embryonic fibroblasts [25], whereas Pds5 depletion did not affect the Esco2-dependent cohesion pathway in HeLa cells. We speculate that the partial disruption of Esco2 localization in the absence of Pds5 is not sufficient to affect its function. Alternatively, there might be a functional difference between Pds5 in human cancer cell lines and mouse embryonic fibroblasts, although it is possible that Pds5 was inactivated to different degrees in the two studies. A more-detailed characterization of Esco2 is required to address these issues.

EXPERIMENTAL PROCEDURES

Cell Culture

HeLa cells were cultured as described [26] and were synchronized using a double-thymidine block: 14–16 hr in the presence of 2 mM thymidine (Sigma), 8 hr release, and 16 hr in the presence of 1.5 mM thymidine. The cells were collected 6–7.5 hr and 13 to 14 hr after the second release for enrichment in G2 and G1, respectively. For the enrichment of cells in prometaphase, nocodazole (100 ng/ml or 400 ng/ml when used in combination with ZM447439) was added 6 hr after release from the second thymidine block, and cells were collected by the shake-off method.

Lentiviral Transduction

Recombinant lentiviruses were produced from 293FT cells transfected with CSII-CMV-Venus (GFP variant)-Esco1 and packaging vectors (RIKEN BioResource Center). HeLa cells were incubated with recombinant lentivirus in the presence of 10 μg/ml polybrene (Sigma).

Antibodies and Reagents

Polyclonal rabbit anti-sororin antibody was generously provided by Dr. J.M. Peters (The Research Institute of Molecular Pathology). Rabbit polyclonal antibody against Rad21 (for ChIP analysis), which was generated using the peptides DEPIIEEPSR and ATPGPRFHII as immunogens, and a rabbit polyclonal antibody against CAPD3 [40] were kindly provided by Dr. T. Hirota (JFCR Cancer Institute). Mouse monoclonal antibodies were raised against the following peptides: Esco1 (CEEKLPVIRSEEEKVRFERQKA),

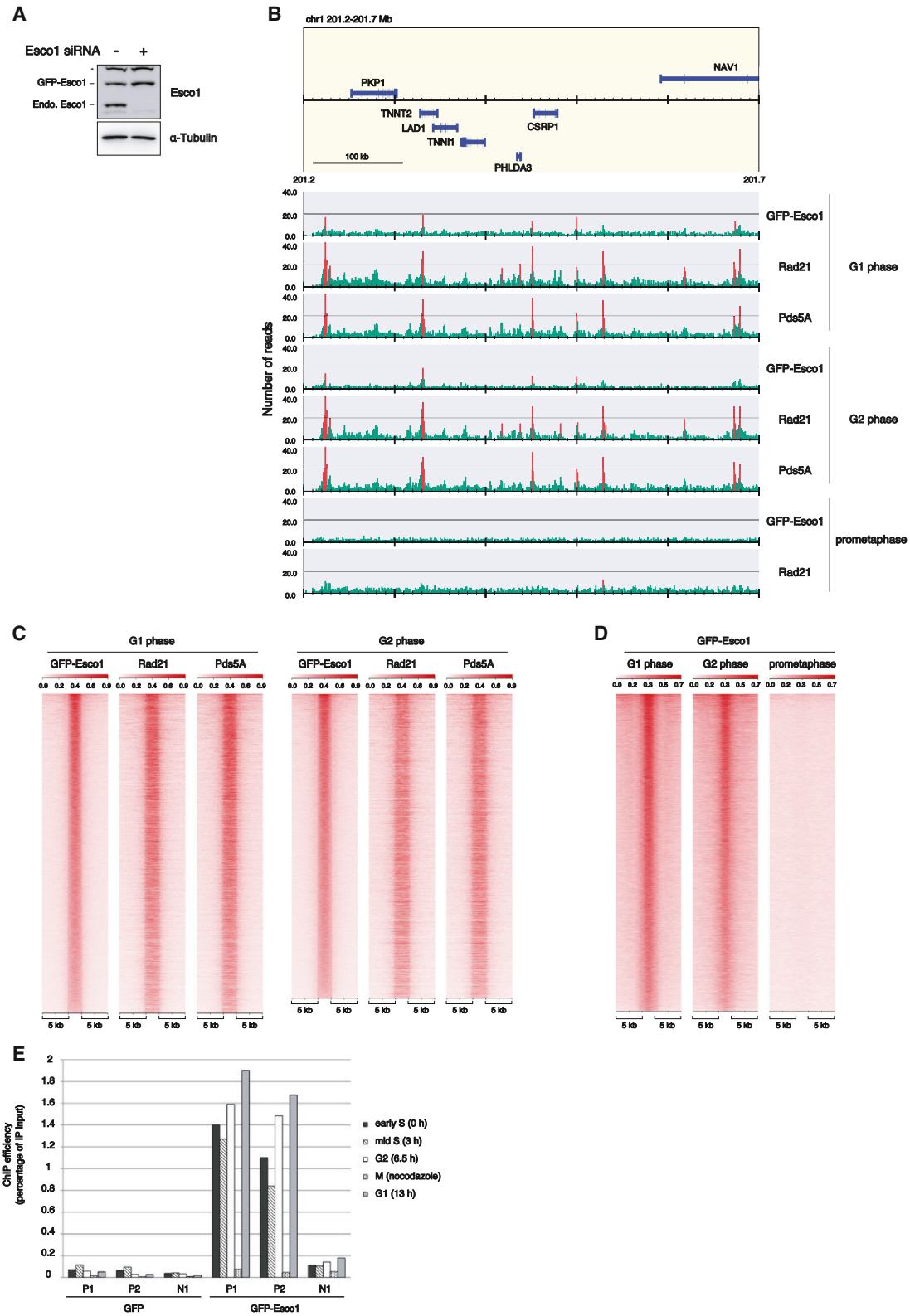

Figure 5. Esco1 Localizes to Cohesin Localization Sites throughout Interphase

(A) Immunoblotting analysis of lysates from cells carrying the GFP-Esco1 in the place of Endo. Esco1. HeLa cells were generated that stably expressed siRNA-resistant versions of wild-type GFP-Esco1. The clone was not transfected (−) or transfected with Esco1 siRNA for 2 days, and lysates from these cells were then analyzed by immunoblotting. Tubulin is shown as a loading control. The asterisk indicates nonspecific signals.

(legend continued on next page)

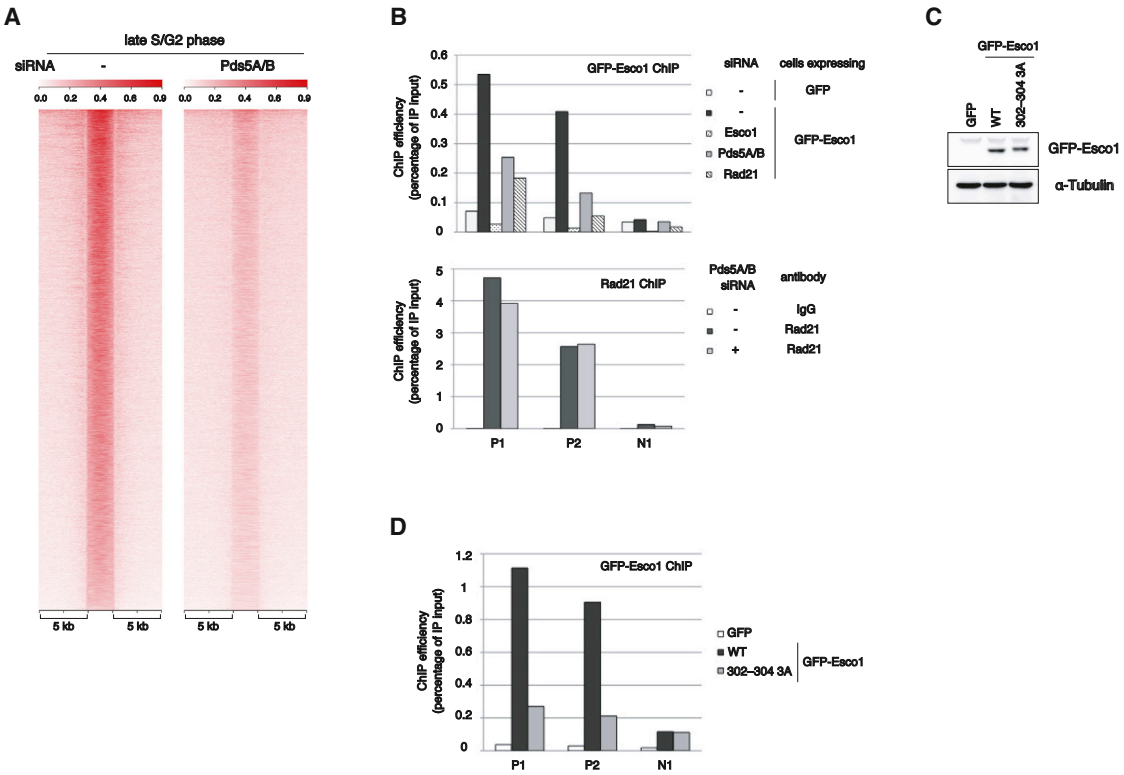

Figure 6. Pds5 Is Essential for Esco1 to Localize to Cohesin Localization Sites

(A) Heatmaps showing ChIP-tag enrichment of GFP-Esco1 in the absence of Pds5 in a window of ±5 kb. This plot is centered on Esco1 peaks, and peaks are ranked by size with the highest peaks at the top of the graph. HeLa cells expressing GFP-Esco1 were transfected with Pds5 siRNAs for 2 days and were then synchronized in G2 by double-thymidine block and release.

(B) ChIP-qPCR data showing the amount of GFP-Esco1 or endogenous Rad21 at the cohesin-positive (P1 and P2) and -negative (N1) sites identified by ChIP-seq. Indicated cells were not transfected (–) or transfected with each siRNA for 2 days and synchronized in S phase. The expression of both endogenous Esco1 and GFP-Esco1 are suppressed by Esco1 siRNA. Chromatin obtained from these cells was immunoprecipitated with anti-GFP or anti-Rad21, and enrichment of GFP-Esco1 and Rad21 was scored by qPCR, respectively. Values are the mean of two PCR amplifications.

(C) Immunoblotting analysis of the expression of WT and 302–304 3A mutant GFP-Esco1 in whole-cell extracts. Tubulin is shown as a loading control.

(D) ChIP-qPCR data showing the relative amount of WT and 302–304 3A mutant GFP-Esco1 at the cohesin-positive (P1 and P2) and -negative (N1) sites identified by ChIP-seq. Cells in (C) were synchronized in G2 by double-thymidine block and release. Chromatin was obtained and immunoprecipitated with anti-GFP. Enrichment of WT and 302–304 3A mutant GFP-Esco1 was scored by qPCR. Values are the mean of two PCR amplifications (see also Figure S6).

pS302 (CEQAGKSKRGpSILQLCEEIA), Esco2 (CSASSKNKEKLIKDSSD DRVSSKEHKVDKNE), Pds5A (CEAGNAKAPKLQDLAKKAAPAERQIDLQR), and Pds5B (MAHSKTRTNDGKITYPPGVKEISDKISKEEMVRRC). The mouse monoclonal antibody against the acetylated form of SMC3 has been described [17]. Commercially obtained antibodies included anti-SMC3 (Abcam and Bethyl Laboratories), anti-SMC1 (Abcam), anti-tubulin (Sigma), M2 antibody recognizing FLAG (Sigma), anti-histone H3 (Abcam), anti-histone H3 S10 phosphorylation (Cell Signaling Technology), anti-Myc (Millipore), anti-His tag (MBL), anti-Wapl (Proteintech Group), anti-Rad21 (for immunoblotting; Millipore), anti-GFP (for immunoprecipitation; Invitrogen), and anti-GFP (for ChIP; Torrey Pines Biolabs). PCI-34051 was synthesized by Synstar Japan. Nocodazole and RO3306 were obtained from Calbiochem, BI2536 was from ChemieTek, and ZM447439 was from TOCRIS Bioscience.

Quantification of Band Intensities in Immunoblotting

Band intensities were quantified using ImageQuant TL software (GE Healthcare). SMC3-ac levels were normalized to SMC1 or SMC3 levels. For the analysis of chromatin association of sororin, sororin levels were normalized to histone H3 levels in chromatin-enriched fraction.

(B) Representative ChIP-seq data (RefSeq gene position 201.2–201.7 Mb of human chromosome 1). Regions in which signals were significantly enriched are shown in red. Binding profiles for GFP-Esco1, Rad21, and Pds5A are shown.

(C) Heatmaps showing ChIP-tag enrichment in the indicated ChIP-seq experiments in a window of ±5 kb around all GFP-Esco1 peaks. Binding profiles in G1 (left) and G2 (right) are shown. Peaks are ranked by size with the highest peaks at the top of the graph.

(D) Heatmaps showing ChIP-tag enrichment of GFP-Esco1 in ChIP-seq experiments with G1, G2, and prometaphase cells in a window of ±5 kb. This plot is centered on GFP-Esco1 peaks observed in G1. Peaks are ranked by size with the highest peaks at the top of the graph.

(E) ChIP-qPCR data showing the relative amounts of GFP-Esco1 at the cohesin-positive (P1 and P2) and -negative (N1) sites identified by ChIP-seq during cell-cycle progression. Cells expressing either GFP or GFP-Esco1 were synchronized at S phase entry by double-thymidine block. After release from the second thymidine arrest, cells were harvested at the indicated time points and cell-cycle profiles were obtained by FACS (Figure S4E). Chromatin was immunoprecipitated with anti-GFP. Enrichment of GFP-Esco1 was scored by qPCR. Values are the mean of two PCR amplifications (see also Figure S5).

RNAi

RNAi was performed as described [26]. The sequences of the stealth siRNAs (Invitrogen) used in this study are Esco1 siRNA (5′-UGAAGUAUUUGUCUUUCAACACUGG-3′), Esco2 no. 1 siRNA (5′-UUUAGGAACAACUUGCUGGAAGCCC-3′), Esco2 no. 2 siRNA (5′-AUAACUUGCCAUCUGGUGUUGGGUC-3′), Esco2 no. 3 siRNA (5′-AUACUUAGCAGUUAAACUCUUCUGU-3′), Pds5A siRNA (5′-UAUUGUUGAUCACUGAGAAGAGAGU-3′ or 5′-AACAGUUAGCCUCUGAUGUAGGCUG-3′), Pds5B siRNA (5′-UUAAUAAGAGCACUGAUAGAUUCGG-3′), sororin siRNA (5′-AACUCCCGAGCAUCCUCCCUGAAAU-3′), and Rad21 siRNA (5′-UUCCACUCUACUCUGAUUCAAGCUG-3′).

Baculovirus Expression System

The cDNA of human Pds5B was obtained from the Kazusa DNA Research Institute. The cDNAs of human Esco1, Esco2, Pds5A, and Pds5B were subcloned into pFastBac-HTB (Invitrogen). Proteins were expressed using the Bac-to-Bac baculovirus expression system (Invitrogen).

Fluorescence-Activated Cell Sorting

Cells were fixed with ethanol, washed with PBS, and stained for DNA with propidium iodine. DNA profiles were analyzed using a FACSCalibur flow cytometer and Cell Quest software (BD Biosciences).

Chromatin Fractionation Analysis for Sororin

Collected cells were washed with PBS and lysed on ice for 10 min in a buffer consisting of 25 mM Tris-HCl (pH 7.5), 250 mM NaCl, 5 mM $MgCl_2$, 10% (v/v) glycerol, 0.2% (v/v) NP-40, 1 mM NaF, 10 mM sodium butyrate, and protease inhibitor cocktail (Complete; Roche). Chromatin-enriched fractions were collected by low-speed centrifugation at 1,500 × *g* for 5 min and were washed with the same buffer.

Immunoprecipitation

For analysis of the Esco-Pds5 interaction, Sf9 cell pellets were resuspended in buffer (25 mM Tris-HCl [pH 7.5], 150 mM NaCl, 10% [v/v] glycerol, 0.2% [v/v] NP-40, and Roche Complete protease inhibitor) for 10 min on ice. After removal of the insoluble fraction by centrifugation at 20,400 × *g* for 15 min, the remainder of each cell extract was used for immunoprecipitation with agarose beads coupled to antibody M2 that recognizes FLAG (Sigma). Precipitates were washed three times with the same buffer.

For the identification of phosphorylation sites in Esco1 by mass spectrometry, GFP-Esco1 was immunoprecipitated from cell extracts of nocodazole-arrested mitotic cells or thymidine-arrested S phase cells. Cells were washed with PBS and then lysed on ice for 15 min in a buffer consisting 25 mM Tris-HCl (pH 7.5), 400 mM NaCl, 0.2% (v/v) NP-40, 10% (v/v) glycerol, and Roche Complete protease inhibitor cocktail. Cell extracts, after removal of the insoluble fraction by centrifugation at 20,400 × *g* for 30 min at 4°C, were used for immunoprecipitation. Protein A Dynabeads (Invitrogen) coupled to anti-GFP (Invitrogen) were incubated with cell extract for 2 hr at 4°C. Precipitates were washed three times with the same buffer and resolved by SDS-PAGE. The gels were stained with Quick-CBB PLUS (Wako Pure Chemical Industries). Protein bands were excised from the gel, digested with Trypsin Gold (Promega) or GluC (New England Biolabs), and analyzed by mass spectrometry.

Chromosome Spreads

HeLa cells were grown asynchronously after siRNA transfection, and mitotic cells were collected by shake-off and hypotonically swollen in a 1:1 solution of PBS and tap water for 5 min at room temperature. Cells were fixed with Carnoy's solution (methanol:acetic acid; 3:1), dropped on glass slides, and dried. Slides were stained with 5% (v/v) Giemsa (Merck), washed with water, air-dried, and mounted with Entellan (Merck).

ChIP-qPCR

ChIP-qPCR was performed as described [26, 29] using the following primers:

P1: F, TAGACGGAGCTGGAAGGAAA
P1: R, AGGGACAGTCACCACCTTTG
P2: F, AAACCTCTGAGCTCATAATGCTG
P2: R, CTGGGTGCAAGCCACACT
P3: F, AAGAAGTCAAGATTTGGTAGCTTTT
P3: R, TCTCCAAGGACTGTGTGCAG
P4: F, GAGAAGAGGTTGTGCCTGGT
P4: R, TGGTTGCTTCTGGTTCACTG
P5: F, CTTGTGAAAGACGGTGCTTG
P5: R, CAGGGGTGAGAGGAAGGAG
N1: F, TTCTGCAACTAGGTAACACC
N1: R, ATAGGTTGGATTACATGATC
N2: F, ACTGTGGCTGGAAGATGAAT
N2: R, TGCCTTTATGATCATTTAGTGAGT

ChIP-Seq and Data Analysis

Deep sequencing of immunoprecipitated chromatin was performed using the Illumina HiSeq 2500 system. Sequencing libraries were made using the NEBNext ChIP-Seq Library Prep Master Mix Set for Illumina (New England Biolabs). Single-end, 50-bp sequence reads for Rad21, Pds5A, and overexpressed GFP-Esco1 or 65-bp sequence reads for GFP-Esco1 with endogenous levels were aligned to the human genome (UCSC hg19) using Bowtie v1.0.0 [41] with the -n3 -m1 option, which reports only unique matches, allowing three mismatches in the first 28 bases per read. All redundant reads (reads starting exactly at the same position) were removed from further analysis. DROMPA v2.5.3 [42] was used for visualization and statistical analysis of ChIP-seq data. For peak-calling, we used PEAKCALL_P command, which tested the significances of the ChIP-read enrichment (Poisson test) and the ChIP/input enrichment (binomial test). We used $p < 10^{-4}$ and $p < 0.05$ for Poisson test and binomial test, respectively. Sequencing, mapping data, and peak calling statistics are summarized in Table S1. Gene annotation was obtained from RefSeq. Heatmaps shown in Figures 5C, 5D, 6A, and S5D were created using ngs.plot [43].

ACCESSION NUMBERS

The accession number for the ChIP-seq data reported in this paper is Sequence Read Archive (SRA) database: SRP056019.

SUPPLEMENTAL INFORMATION

Supplemental Information includes six figures and one table and can be found with this article online at http://dx.doi.org/10.1016/j.cub.2015.05.017.

AUTHOR CONTRIBUTIONS

M.M., M.B., and K.S. designed the experiments. M.M. performed biochemical analyses and prepared chromosome spreads under the guidance of M.B. M.M., M.I., R.N., K.A., M.B., Y.K., and K.S. performed the ChIP-seq and analysis. T.H. isolated the antibody against Rad21. M.M., M.B., M.I., R.N., T.S., L.N., H.T., and K.S. interpreted the data, and M.M., M.B., T.S., and K.S. drafted the manuscript.

ACKNOWLEDGMENTS

We are grateful to J.M. Peters for anti-sororin antibody and to T. Nishiyama for discussions. This work was supported by Grants-in-Aid for Scientific Research (category S) to K.S., on Innovative Areas to K.S., and category B to M.B.

Received: November 13, 2014
Revised: April 8, 2015
Accepted: May 8, 2015
Published: June 4, 2015

REFERENCES

1. Guacci, V., Koshland, D., and Strunnikov, A. (1997). A direct link between sister chromatid cohesion and chromosome condensation revealed through the analysis of MCD1 in S. cerevisiae. Cell *91*, 47–57.

2. Michaelis, C., Ciosk, R., and Nasmyth, K. (1997). Cohesins: chromosomal proteins that prevent premature separation of sister chromatids. Cell *91*, 35–45.
3. Haering, C.H., Farcas, A.-M., Arumugam, P., Metson, J., and Nasmyth, K. (2008). The cohesin ring concatenates sister DNA molecules. Nature *454*, 297–301.
4. Nasmyth, K., and Haering, C.H. (2009). Cohesin: its roles and mechanisms. Annu. Rev. Genet. *43*, 525–558.
5. Peters, J.-M., and Nishiyama, T. (2012). Sister chromatid cohesion. Cold Spring Harb. Perspect. Biol. *4*, pii: a011130.
6. Rowland, B.D., Roig, M.B., Nishino, T., Kurze, A., Uluocak, P., Mishra, A., Beckouët, F., Underwood, P., Metson, J., Imre, R., et al. (2009). Building sister chromatid cohesion: smc3 acetylation counteracts an antiestablishment activity. Mol. Cell *33*, 763–774.
7. Zhang, J., Shi, X., Li, Y., Kim, B.-J., Jia, J., Huang, Z., Yang, T., Fu, X., Jung, S.Y., Wang, Y., et al. (2008). Acetylation of Smc3 by Eco1 is required for S phase sister chromatid cohesion in both human and yeast. Mol. Cell *31*, 143–151.
8. Unal, E., Heidinger-Pauli, J.M., Kim, W., Guacci, V., Onn, I., Gygi, S.P., and Koshland, D.E. (2008). A molecular determinant for the establishment of sister chromatid cohesion. Science *321*, 566–569.
9. Rolef Ben-Shahar, T., Heeger, S., Lehane, C., East, P., Flynn, H., Skehel, M., and Uhlmann, F. (2008). Eco1-dependent cohesin acetylation during establishment of sister chromatid cohesion. Science *321*, 563–566.
10. Ivanov, D., Schleiffer, A., Eisenhaber, F., Mechtler, K., Haering, C.H., and Nasmyth, K. (2002). Eco1 is a novel acetyltransferase that can acetylate proteins involved in cohesion. Curr. Biol. *12*, 323–328.
11. Milutinovich, M., Unal, E., Ward, C., Skibbens, R.V., and Koshland, D. (2007). A multi-step pathway for the establishment of sister chromatid cohesion. PLoS Genet. *3*, e12.
12. Tóth, A., Ciosk, R., Uhlmann, F., Galova, M., Schleiffer, A., and Nasmyth, K. (1999). Yeast cohesin complex requires a conserved protein, Eco1p(Ctf7), to establish cohesion between sister chromatids during DNA replication. Genes Dev. *13*, 320–333.
13. Skibbens, R.V., Corson, L.B., Koshland, D., and Hieter, P. (1999). Ctf7p is essential for sister chromatid cohesion and links mitotic chromosome structure to the DNA replication machinery. Genes Dev. *13*, 307–319.
14. Bellows, A.M., Kenna, M.A., Cassimeris, L., and Skibbens, R.V. (2003). Human EFO1p exhibits acetyltransferase activity and is a unique combination of linker histone and Ctf7p/Eco1p chromatid cohesion establishment domains. Nucl. Acids Res *31*, 6334–6343.
15. Hou, F., and Zou, H. (2005). Two human orthologues of Eco1/Ctf7 acetyltransferases are both required for proper sister-chromatid cohesion. Mol. Biol. Cell *16*, 3908–3918.
16. Whelan, G., Kreidl, E., Wutz, G., Egner, A., Peters, J.-M., and Eichele, G. (2012). Cohesin acetyltransferase Esco2 is a cell viability factor and is required for cohesion in pericentric heterochromatin. EMBO J. *31*, 71–82.
17. Nishiyama, T., Ladurner, R., Schmitz, J., Kreidl, E., Schleiffer, A., Bhaskara, V., Bando, M., Shirahige, K., Hyman, A.A., Mechtler, K., and Peters, J.M. (2010). Sororin mediates sister chromatid cohesion by antagonizing Wapl. Cell *143*, 737–749.
18. Uhlmann, F., and Nasmyth, K. (1998). Cohesion between sister chromatids must be established during DNA replication. Curr. Biol. *8*, 1095–1101.
19. Lengronne, A., McIntyre, J., Katou, Y., Kanoh, Y., Hopfner, K.-P., Shirahige, K., and Uhlmann, F. (2006). Establishment of sister chromatid cohesion at the S. cerevisiae replication fork. Mol. Cell *23*, 787–799.
20. Moldovan, G.-L., Pfander, B., and Jentsch, S. (2006). PCNA controls establishment of sister chromatid cohesion during S phase. Mol. Cell *23*, 723–732.
21. Song, J., Lafont, A., Chen, J., Wu, F.M., Shirahige, K., and Rankin, S. (2012). Cohesin acetylation promotes sister chromatid cohesion only in association with the replication machinery. J. Biol. Chem. *287*, 34325–34336.
22. Noble, D., Kenna, M.A., Dix, M., Skibbens, R.V., Ünal, E., and Guacci, V. (2006). Intersection between the regulators of sister chromatid cohesion establishment and maintenance in budding yeast indicates a multi-step mechanism. Cell Cycle *5*, 2528–2536.
23. Vaur, S., Feytout, A., Vazquez, S., and Javerzat, J.-P. (2012). Pds5 promotes cohesin acetylation and stable cohesin-chromosome interaction. EMBO Rep. *13*, 645–652.
24. Chan, K.-L., Gligoris, T., Upcher, W., Kato, Y., Shirahige, K., Nasmyth, K., and Beckouët, F. (2013). Pds5 promotes and protects cohesin acetylation. Proc. Natl. Acad. Sci. USA *110*, 13020–13025.
25. Carretero, M., Ruiz-Torres, M., Rodríguez-Corsino, M., Barthelemy, I., and Losada, A. (2013). Pds5B is required for cohesion establishment and Aurora B accumulation at centromeres. EMBO J. *32*, 2938–2949.
26. Deardorff, M.A., Bando, M., Nakato, R., Watrin, E., Itoh, T., Minamino, M., Saitoh, K., Komata, M., Katou, Y., Clark, D., et al. (2012). HDAC8 mutations in Cornelia de Lange syndrome affect the cohesin acetylation cycle. Nature *489*, 313–317.
27. Lengronne, A., Katou, Y., Mori, S., Yokobayashi, S., Kelly, G.P., Itoh, T., Watanabe, Y., Shirahige, K., and Uhlmann, F. (2004). Cohesin relocation from sites of chromosomal loading to places of convergent transcription. Nature *430*, 573–578.
28. Glynn, E.F., Megee, P.C., Yu, H.-G., Mistrot, C., Unal, E., Koshland, D.E., DeRisi, J.L., and Gerton, J.L. (2004). Genome-wide mapping of the cohesin complex in the yeast Saccharomyces cerevisiae. PLoS Biol. *2*, E259.
29. Wendt, K.S., Yoshida, K., Itoh, T., Bando, M., Koch, B., Schirghuber, E., Tsutsumi, S., Nagae, G., Ishihara, K., Mishiro, T., et al. (2008). Cohesin mediates transcriptional insulation by CCCTC-binding factor. Nature *451*, 796–801.
30. Sumara, I., Vorlaufer, E., Gieffers, C., Peters, B.H., and Peters, J.-M. (2000). Characterization of vertebrate cohesin complexes and their regulation in prophase. J. Cell Biol. *151*, 749–762.
31. Waizenegger, I.C., Hauf, S., Meinke, A., and Peters, J.M. (2000). Two distinct pathways remove mammalian cohesin from chromosome arms in prophase and from centromeres in anaphase. Cell *103*, 399–410.
32. Losada, A., Hirano, M., and Hirano, T. (2002). Cohesin release is required for sister chromatid resolution, but not for condensin-mediated compaction, at the onset of mitosis. Genes Dev. *16*, 3004–3016.
33. Unal, E., Heidinger-Pauli, J.M., and Koshland, D. (2007). DNA double-strand breaks trigger genome-wide sister-chromatid cohesion through Eco1 (Ctf7). Science *317*, 245–248.
34. Ström, L., Karlsson, C., Lindroos, H.B., Wedahl, S., Katou, Y., Shirahige, K., and Sjögren, C. (2007). Postreplicative formation of cohesion is required for repair and induced by a single DNA break. Science *317*, 242–245.
35. Heidinger-Pauli, J.M., Unal, E., and Koshland, D. (2009). Distinct targets of the Eco1 acetyltransferase modulate cohesion in S phase and in response to DNA damage. Mol. Cell *34*, 311–321.
36. Kim, B.-J., Li, Y., Zhang, J., Xi, Y., Li, Y., Yang, T., Jung, S.Y., Pan, X., Chen, R., Li, W., et al. (2010). Genome-wide reinforcement of cohesin binding at pre-existing cohesin sites in response to ionizing radiation in human cells. J. Biol. Chem. *285*, 22784–22792.
37. Seitan, V.C., and Merkenschlager, M. (2012). Cohesin and chromatin organisation. Curr. Opin. Genet. Dev. *22*, 93–100.
38. Schmitz, J., Watrin, E., Lénárt, P., Mechtler, K., and Peters, J.-M. (2007). Sororin is required for stable binding of cohesin to chromatin and for sister chromatid cohesion in interphase. Curr. Biol. *17*, 630–636.

39. Vega, H., Waisfisz, Q., Gordillo, M., Sakai, N., Yanagihara, I., Yamada, M., van Gosliga, D., Kayserili, H., Xu, C., Ozono, K., et al. (2005). Roberts syndrome is caused by mutations in ESCO2, a human homolog of yeast ECO1 that is essential for the establishment of sister chromatid cohesion. Nat. Genet. *37*, 468–470.

40. Abe, S., Nagasaka, K., Hirayama, Y., Kozuka-Hata, H., Oyama, M., Aoyagi, Y., Obuse, C., and Hirota, T. (2011). The initial phase of chromosome condensation requires Cdk1-mediated phosphorylation of the CAP-D3 subunit of condensin II. Genes Dev. *25*, 863–874.

41. Langmead, B., Trapnell, C., Pop, M., and Salzberg, S.L. (2009). Ultrafast and memory-efficient alignment of short DNA sequences to the human genome. Genome Biol. *10*, R25.

42. Nakato, R., Itoh, T., and Shirahige, K. (2013). DROMPA: easy-to-handle peak calling and visualization software for the computational analysis and validation of ChIP-seq data. Genes Cells *18*, 589–601.

43. Shen, L., Shao, N., Liu, X., and Nestler, E. (2014). ngs.plot: Quick mining and visualization of next-generation sequencing data by integrating genomic databases. BMC Genomics *15*, 284.

